A *Chandra* X-ray Survey of Ultraluminous Infared Galaxies

S.H. Teng, A.S. Wilson, S. Veilleux (U.Md), A.J. Young (MIT), D.B. Sanders (U. Hawaii), N.M. Nagar (Kapteyn Inst. & U. de Concepción)

Abstract

We present results from *Chandra* observations of 14 ultraluminous infrared galaxies (ULIRGs; $L_{IR} \geq 10^{12}$ L_{sun} with H_0 = 75 km s^{-1} Mpc^{-1}, q_0=0) with redshifts between 0.04 and 0.16. The goals of the observations were to investigate any correlation between infrared color or luminosity and the properties of the X-ray emission and to attempt to determine whether these objects are powered by starbursts or active galactic nuclei (AGNs). The sample contains approximately the same number of high- and low-luminosity objects and "warm" and "cool" ULIRGs. All 14 galaxies were detected by *Chandra*.

Introduction

- **Why observe ULIRGs?**
  - Observations have shown that almost all ULIRGs are undergoing mergers
  - Galactic mergers are thought to be progenitors of some elliptical galaxies and may be a phase through which galaxies pass before a quasar is formed
  - Similar to submillimeter sources at z=1-4 observed with SCUBA
  - May account for most or all of the submillimeter/far-infrared background, as a result of the strong cosmological evolution
- **What do we want to know?**
  - Whether the high luminosity of these galaxies result from starburst or accretion onto supermassive black holes?
  - Is the evolutionary sequence of merger-induced starburst ("cool" ULIRGs) to "warm ULIRGs" to QSOs true, since "warm" ULIRGs tend to have Seyfert-like optical and near-infrared spectra?
- **Why observe in X-rays?**
  - Nuclei of ULIRGs may be very heavily obscured
  - Radio observations can only detect the presence of an AGN
  - Bolometric luminosity in the radio band is insignificant, thus cannot prove that accretion is the dominant energy source
  - Pure starbursts, at low redshifts, do not exhibit unresolved hard X-ray nuclei
  - If the column density is high, dust can attenuate directly viewed X-rays from an AGN. In this case, the detection of an Fe Kα line of large equivalent width may be the best determinant of an energetically dominant AGN.
- **How does this survey differ from others?**
  - Ptak et al. (2003) observed ULIRGs with *Chandra*, but their sample was volume limited (z < 0.045)
  - Franceschini et a. (2003) observed with *XMM* and included only the brightest nearby ULIRGs with one ULIRG with z > 0.082
  - Our sample includes ULIRGs with 0.04 < z < 0.16 and is selected to cover uniformly the *IRAS* color-luminosity plane (see Fig. 1)

Figure 1:
Distribution of the 1 Jy sample ULIRGs in the IRAS flux vs. luminosity plane. The letters represent optical spectral type classifications of ULIRGs (S = Seyferts, L = LINERs, H = HII galaxies) observed previously and in this work. The uppercase letters represent spectral types of our sample, while the lowercase letters represent spectral types of ULIRGs observed by Ptak et al. (2003) and Franceschini et al. (2003). Note that three of the galaxies in our sample have been previously observed by the other two groups. The horizontal dotted line denotes the separation between "warm" and "cool" ULIRGs, while the vertical dotted line denotes the separation of high and low luminosity ULIRGs.
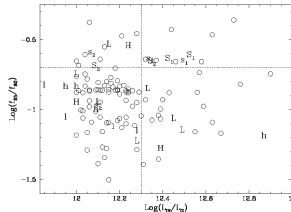
Sample Selection

- Objects were selected from the *IRAS* 1-Jy sample of ULIRGs (Kim and Sanders, 1998; Veilleux et al. 1999a,b; Kim et al. 2002; Veilleux et al. 2002).
- Objects are distributed approximately equally in the *IRAS* color vs. luminosity plane, so that the sample adequately tests the full range of infrared luminosities and infrared colors that characterize the class of ULIRGs. (Fig. 1)
- The distribution of sources allows us to test whether objects with certain infrared colors and luminosities are powered preferentially by stars or by AGNs.

Source name	Spectral type	z	NH (Galactic) (10^{20} cm^{-2})	Exposure (GTI, in ks)	Total counts	Hardness ratio	Γ^1 (estimated)	kT^1 (keV) (estimated)
F00188-0856	LINER	0.128	3.21	9.80	16	$-0.25^{+0.36}_{-0.25}$	$1.1^{+0.5}_{-0.6}$	79.9^{+--}_{-73}
F01004-2237	H II	0.118	1.58	9.40	20	$-0.40^{+0.32}_{-0.24}$	$1.4^{+0.6}_{-0.6}$	15.8^{+62}_{-12}
F01572+0009	Seyfert 1	0.163	2.56	10.60	4386	$-0.69^{+0.02}_{-0.02}$	$2.17^{+0.10}_{-0.07}$	$2.8^{+0.2}_{-0.2}$
Z03521+0028	LINER	0.152	12.5	7.20	3	$-0.33^{+1.23}_{-0.54}$	$1.5^{+1.9}_{-3.4}$	12.6^{+65}_{-11}
F04103-2838	LINER	0.118	2.45	10.00	30	$-0.20^{+0.24}_{-0.18}$	$1.05^{+0.35}_{-0.45}$	79.9^{+--}_{-61}
F10190+1322	H II	0.077	3.78	9.40	16	$-0.25^{+0.36}_{-0.25}$	$1.18^{+0.50}_{-0.68}$	79.9^{+--}_{-73}
Z11598-0112	Seyfert 1	0.151	2.25	10.20	1481	$-0.82^{+0.03}_{-0.03}$	$2.7^{+0.2}_{-0.1}$	$1.8^{+0.2}_{-0.2}$
F12072-0444	Seyfert 2	0.129	3.32	9.20	16	$-0.75^{+0.43}_{-0.25}$	$2.5^{+0.6}_{-1.1}$	$2.0^{+48}_{-1.7}$
F12112+0305	LINER	0.073	1.75	10.00	51	$-0.45^{+0.19}_{-0.15}$	$1.5^{+0.4}_{-0.4}$	$7.9^{+7.4}_{-3.9}$
F15130-1958	Seyfert 2	0.109	8.60	9.80	38	$-0.63^{+0.24}_{-0.18}$	$2.15^{+0.75}_{-0.6}$	$3.2^{+5.7}_{-1.4}$
F15250+3609[2]	LINER	0.055	1.56	9.20	37	$-0.73^{+0.25}_{-0.21}$	$2.27^{+1.24}_{-0.77}$	$2.5^{+5.4}_{-1.4}$
F16090-0139	LINER	0.134	9.25	9.80	27	$-0.41^{+0.23}_{-0.18}$	$1.57^{+0.53}_{-0.45}$	$7.9^{+72}_{-4.7}$
F17208-0014[2]	H II	0.043	9.96	8.60	92	$-0.35^{+0.13}_{-0.11}$	$1.43^{+0.27}_{-0.23}$	$11.2^{+69}_{-5.6}$
F23365+3604[2]	LINER	0.064	9.36	10.20	34	$-0.18^{+0.22}_{-0.17}$	$1.10^{+0.35}_{-0.25}$	79.9^{+--}_{-68}

[1] Values estimated from hardness ratio fits. [2] Denotes objects not in 1-Jy sample

Data Reduction Techniques

- **Bright sources**
  - 2 sources were bright enough for traditional spectral fitting
  - Single power law models underestimate the flux at soft energies (0.5-2.0 keV)
  - Modeled data using 2 power laws or power law + MEKAL assuming solar abundances and absorption from only the Galaxy
  - Binned data to at least 15 cts bin^{-1} and 3 cts bin^{-1}; fit spectra using χ^2 or Cash statistics
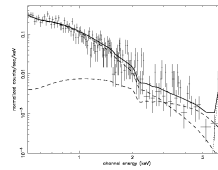 - Spectrum of Z11598-0112 shows hint of emission at the Fe Kα range (Fig. 2)

Figure 2: Spectrum of Z11598-0112 with data binned to 3 cts bin^{-1}. Note the Fe Kα emission at a rest energy of 7.0 keV. The line is significant at a 99% confidence level.
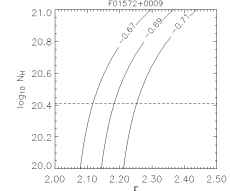
Figure 3: Sample hardness ratio fit. The nominal photon index (or MEKAL temperature) is estimated from this plot assuming Galactic column density.

- **Faint sources**
  - Too few counts for traditional spectral fitting
  - Used hardness ratios to estimate photon index (Γ) of single power law and MEKAL temperature (Fig. 3, estimated fit results in Table)
  - Assumed solar abundances and Galactic column density
  - Tested method by comparing results from bright source fits
  - Used estimated photon index to approximate X-ray luminosity

Summary of Results

- **At least two of the fourteen sources are AGN dominated.**
- **Bright Sources (F01572+0009 and Z11598-0112):**
  - Unresolved nuclear soft X-ray emission; F01572+0009 may be slightly extended
  - Best-fit MEKAL model for the soft component has kT ~250 eV, lower than expected from similar models applied to starbursts (~600 eV) by Ptak et al. (1999)
  - Hard X-ray to bolometric flux ratios similar to those of PG quasars
  - Star formation rate from X-ray flux exceeds SFR estimated from IR flux
  - X-ray to far-infrared ratio near those of AGNs and composites. (Fig. 4)
- **Faint Sources:**
  - Soft X-ray flux to infrared flux ratio suggests starburst dominance
  - Possible emission processes
    - *X-ray binaries*
      - Histogram of photon indices from our sample and the Ptak et al. sample peak at 1-1.4, similar to average Γ value of HMXBs (Fig. 5)
      - LMXBs do not contribute significantly to X-ray luminosity (~3% of SFR)
    - *Thermal bremsstrahlung*
      - Rupke et al. (2005a,b,c) have shown evidence of galactic winds in the 1-Jy sample
      - Spectrum of thermal bremsstrahlung has Γ~1.2 for E ≤ kT, coincides with peak in histogram (Fig. 5)
    - *Absorbed AGN*
      - If column density is high enough, absorption will become important
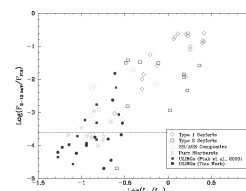   - Compton-thick AGNs have been detected in several ULIRGs

Figure 4: ULIRGs amongst starbursts and composites. Plot reproduced from Ptak et al. (2003) and includes our data. The dotted line represents the average X-ray to far-infrared flux ratio for starbursts.
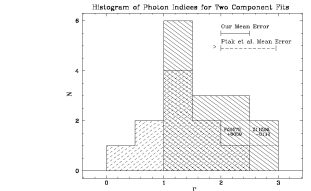
Figure 5: Histogram of photon indices. Plot includes data from this work (solid hashes) and Ptak et al. (2003) values (dashed hashes). Photon indices of the two AGN dominated ULIRGs in our sample are identified.

This work will appear in the Astrophysical Journal. (Teng et al. 2005, ApJ, 633, 664)